Progress In Electromagnetics Research C, Vol. 138, 105–116, 2023

Method for Calculating True Value of Landslide Deformation Based on Micro Deformation Monitoring Radar

Yaolong Qi[1, 2], Lei Zhang[1, 2, *], Weixian Tan[1, 2], Pingping Huang[1, 2], Zhonggen Wei[3, 4], and Haikun Liu[1, 2]

Abstract—Micro Deformation Monitoring Radar has been widely used in the field of surface deformation and displacement monitoring. However, limited by radar imaging geometry, the deformation measurement by existing radar technology can only extract the deformation and displacement of the target line of sight (LoS), which cannot directly reflect the actual deformation and displacement of the landslide direction and easily results in misjudgment or omission of the surface deformation monitoring information. In this paper, the relationship model and mapping between radar data and three-dimensional coordinate system were analyzed to perform three-dimensional analysis of the LoS displacement. Combined with the landslide displacement direction, the mapping angle between the LoS direction at any point in the observation area and the landslide direction was solved, and then the deformation displacement in the landslide direction was obtained by solving the LoS direction displacement. Finally, taking the measured data of one slope as the research object, the feasibility and accuracy of the method were analyzed and verified. The conclusion shows that the method proposed in this paper can be effectively applied to calculate the true value of landslide deformation.

1. INTRODUCTION

China is a country with frequent landslide disasters, which poses a serious threat to human life and may cause serious losses in property, infrastructure, and environmental degradation. For example, on March 15, 2019, a landslide occurred in Xiangning County, Linfen City, Shanxi Province, resulting in 20 deaths and 13 injuries, and a direct economic loss of 7.135 million yuan. According to the statistical data released by the Geological Disaster Technical Guidance Center of the Ministry of Natural Resources, there were 6181 geological disasters in 2019, including 4220 landslides, accounting for 68.27% of the total number of geological disasters [1, 2]. The early prevention, monitoring, and prediction of landslides have always been a common concern. At present, the calculation of deformation displacement in the direction of landslide mainly depends on the single-point high-precision measurement method. However, this method must be deployed to the site, and the network must be selected. It is difficult to meet the monitoring requirements for the personnel who cannot set foot in the wide area and large area. Especially when the calculation of deformation displacement needs to estimate the landslide direction, it is unable to effectively grasp the macroscopic trend of surface deformation [3–5].

The micro-variable monitoring radar benefits from its all-weather imaging ability and has the advantages of wide observation area, high accuracy, high resolution, and areas that cannot be accessed by non-contact monitoring personnel. It effectively makes up for the shortcomings of traditional monitoring

Received 20 March 2023, Accepted 9 August 2023, Scheduled 5 October 2023

* Corresponding author: Lei Zhang (349339901@qq.com).

[1] College of Information Engineering, Inner Mongolia University of Technology, Hohhot, Inner Mongolia 010051, China. [2] Inner Mongolia Key Laboratory of Radar Technology and Application, Hohhot, Inner Mongolia 010051, China. [3] China Coal Technology and Engineering Group Shenyang Research Institute, Fushun 113122, China. [4] State Key Laboratory of Coal Mine Safety Technology, Fushun 113122, China.

methods such as Limited spatial range, low density of monitoring points, and difficulty to implement monitoring in dangerous areas. However, due to the characteristics of the micro-variation monitoring radar, it can only obtain the displacement of the radar line of sight through monitoring. Only when the landslide deformation direction is consistent with the LoS direction can it accurately reflect the true deformation displacement of the landslide direction. However, most of the conditions do not meet the above conditions, and the monitoring results are not enough to reflect the true displacement of the target [6–9]. At present, under the condition of a single data source (without the introduction of ascent/descent orbit and multi-platform data), differential interferometry synthetic aperture radar (DINSAR) obtains the deformation vector along the flight direction of the satellite based on pixel offset estimation (Offset-tracking), multiple aperture interferometry (MAI) and other technologies to achieve more comprehensive information acquisition based on SAR images [10]. There is little research on ground-based micro-variation monitoring radar in this area. Some researchers have realized the multi-aperture interferometry technology used for spaceborne SAR on ground-based SAR and successfully obtained the two-dimensional displacement of the target [11, 12]. In this paper, the angles among the three projection components of the LoS-direction deformation and the due east, due north, and due up directions are determined by three-dimensional spatial geographic coordinates, and the mapping angle between the LoS-direction displacement and the landslide deformation direction is calculated by combining the landslide displacement direction. Finally, the true value of the landslide deformation is calculated by the mapping relationship between the radar LoS-direction displacement and the landslide deformation direction.

2. PRINCIPLE OF INTERFEROMETRY

2.1. Deformation Monitoring Model

The ground-based micro-variation monitoring radar adopts fixed orbit. Compared with the airborne and spaceborne InSAR processing process, the steps of baseline estimation, ground leveling effect, and orbit redefinition can be omitted [13]. As shown in Figure 1, O is the midpoint of the radar orbit. In two observations, the distance from the radar to any point of target P changes as $r_{\text{defo}} = R_1 - R_2$. The change is proportional to the interference phase of the two images, and the deformation information can be extracted through the interference phase.

Through the phase information in the echo signal, the relationship between the phase ϕ and skew

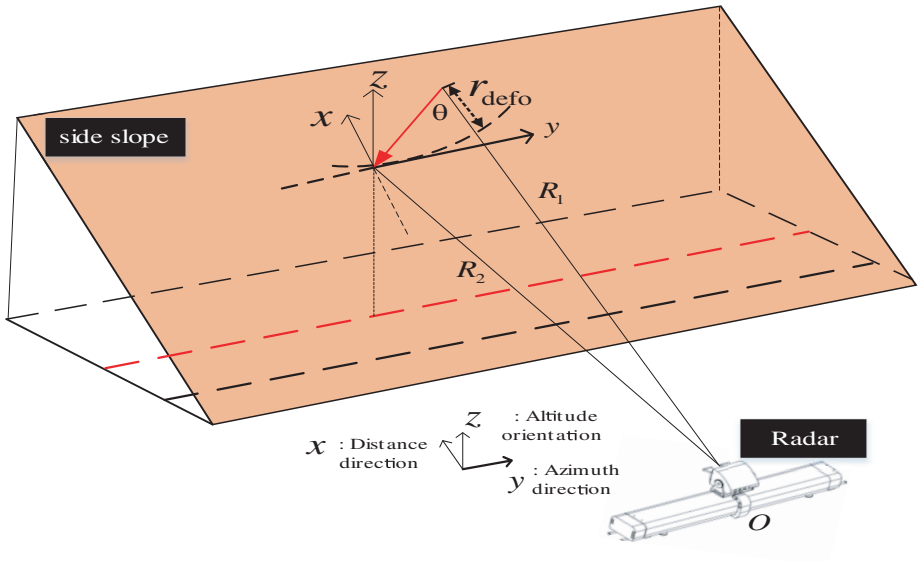

Figure 1. Schematic diagram of Micro Deformation Monitoring radar deformation extraction.

R distance is obtained as follows:

$$\phi = -\frac{4\pi}{\lambda}R \tag{1}$$

where λ is the wavelength of the radar transmitted signal, and the scattering phase difference after deformation is $\Delta\phi$.

$$\Delta\phi = \phi_1 - \phi_2 = -\frac{4\pi}{\lambda}(R_1 - R_2) \tag{2}$$

The relationship between differential phase and deformation value is obtained as follows:

$$\Delta\phi = \phi_1 - \phi_2 = -\frac{4\pi}{\lambda}(R_1 - R_2) = -\frac{4\pi}{\lambda}r_{\text{defo}} \tag{3}$$

So we can get the skew distance difference before and after the target deformation:

$$\mathrm{r}_{\text{defo}} = (R_1 - \mathrm{R}_2) = -\frac{\lambda}{4\pi}\Delta\phi \tag{4}$$

2.2. Deformation Decomposition Model

When the radar is far from the measured target, the two radar waves are approximately parallel, as shown in Figure 2. The parameter r shows the actual deformation. R_1 and R_2 are the skew lengths before and after deformation, and angle θ is the mapping angle between the true value of deformation and the LoS displacement. The calculation of the true value of landslide deformation in the direction of landslide can be expressed as formula (5) by assuming the geometric relationship of approximate parallel slope distance. The calculation of the true value of landslide deformation is related to angle θ.

$$r = \frac{r_{\text{defo}}}{\cos\theta} \tag{5}$$

$$\theta = \arccos\left(\frac{\overrightarrow{PP'}\cdot\overrightarrow{PO}}{\left|\overrightarrow{PP'}\right|\cdot\left|\overrightarrow{PO}\right|}\right) \tag{6}$$

In formula (6), the coordinates of any point P and radar center point O can be determined by three-dimensional space coordinates, and $\overrightarrow{PP'}$ is the main sliding displacement direction of the landslide. The determination method will be described in detail later. According to the precise relationship in Figure 1, the LoS-direction displacement $r_{\text{defo}} = R_1 - R_2$ of any point P in the observation area detected

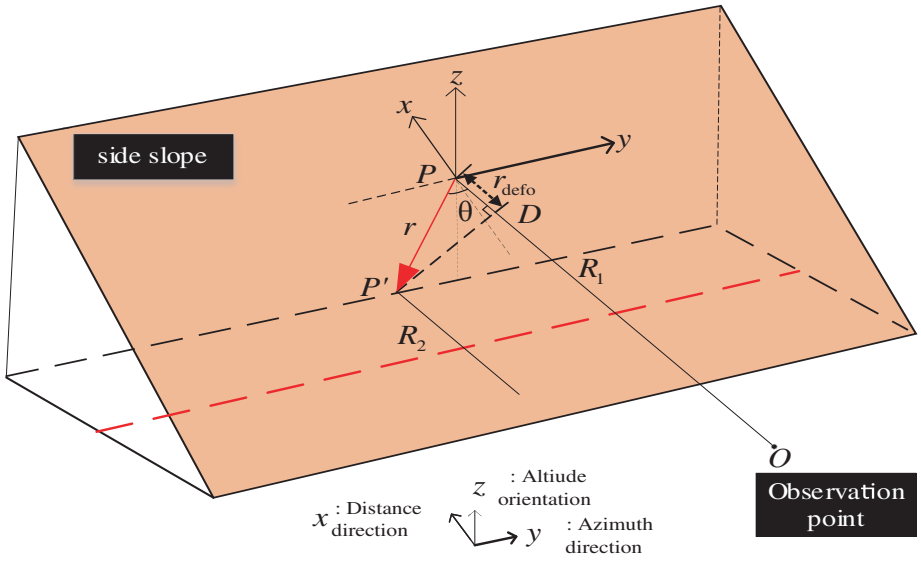

Figure 2. Slope distance approximate parallel hypothesis geometric relationship.

by the radar can be obtained by using the cosine theorem. The relationship between the LoS-direction displacement and landslide direction can be obtained as shown in Formula (7) [14]. The expression of the true value of deformation can be obtained by solving the equation as shown in Formula (8). The deformation displacement in the landslide direction is related to the slope distance R_2, mapping angle θ, and interference phase ϕ.

$$R_2^2 = (R_1 - r_{\text{defo}})^2 = r^2 + R_1^2 - 2rR_1\cos\theta \tag{7}$$

$$r = R_1\cos\theta \pm \sqrt{R_1^2\cos^2\theta + r_{\text{defo}}^2 - 2R_1 r_{\text{defo}}} \tag{8}$$

The calculation of deformation displacement in landslide direction changes correspondingly according to the size of the mapping angle θ. In the formula, when $\theta \in (0^\circ, 90^\circ)$ is a positive sign and when $\theta \in (90^\circ, 180^\circ)$ is a negative sign, when the mapping angle θ is 0°, the apparent displacement is the true value of landslide deformation. When the mapping angle θ is close to 90°, the radar almost loses its monitoring ability. Therefore, in actual monitoring, the included angle between the radar line of sight and the slope should be as small as possible, taking into account the acquisition of sufficient scattering characteristics of the measured target.

3. MAIN SLIDING DIRECTION ALONG THE SLOPE

The determination of landslide displacement direction is relatively complex and is often determined according to the landform. Generally, the main sliding direction of the landslide is the line between the highest and most convex point on the back wall, the farthest and outermost convex point pushed out by the front edge of the landslide mass, and the deepest point on the upper and lower concave of the cross section after the landslide. In addition, through displacement monitoring, the plane resultant displacement vector curve of the landslide in a period of time can be obtained to determine the direction of the landslide. When the vast majority of slopes are unstable, the direction of the landslide is basically consistent with the slope inclination. As a non-contact monitoring method, micro-variation monitoring radar can obtain high-resolution radar images and million-level monitoring points through spatial scanning. Therefore, the use of micro-variation monitoring radar can obtain the main sliding direction information of landslide more conveniently and accurately.

In this paper, the momentum gradient descent method is introduced to determine the main sliding direction of landslides by solving the gradient of deformation scalar field. Firstly, the deformation data and 3D terrain data are fused, and then the pixel with the largest cumulative deformation variable or deformation velocity is selected as the initial point, and then the local surface fitting is performed to obtain the objective function. Finally, the momentum gradient descent method is used to identify and judge the main sliding direction.

3.1. Data Acquisition

The micro-variation monitoring radar data can provide high-precision, real-time and regional change data, and the visualization effect of its monitoring results is insufficient. In order to make full use of the relationship between the data and take full account of the uniqueness of the data to improve the accuracy of the decision results, it is necessary to register and integrate the 3D terrain data and the monitoring results of the micro-variation monitoring radar in a unified coordinate system. As shown in Figure 3, in this paper, the point cloud data obtained by the tilt camera system is processed to generate the three-dimensional figure of the target slope. Combined with geographical coordinates, it can accurately locate the position of each observation area and then integrate the deformation data of the micro-variation monitoring radar with it to realize the three-dimensional visual display of the observation area and cross-validation of accuracy.

The monitoring results of linear scanning synthetic-aperture (LSA) radar system of micro-variation monitoring radar and the results of unmanned aerial vehicle (UAV) 3D image fusion are shown in Figure 4. Using the UAV photographic image to obtain the ultra-high resolution real surface information of the observation area and the 3D point cloud data of the observation area, the 3D spatial geographic coordinates of any observation point P and radar center O in the observation area can be obtained [15, 16].

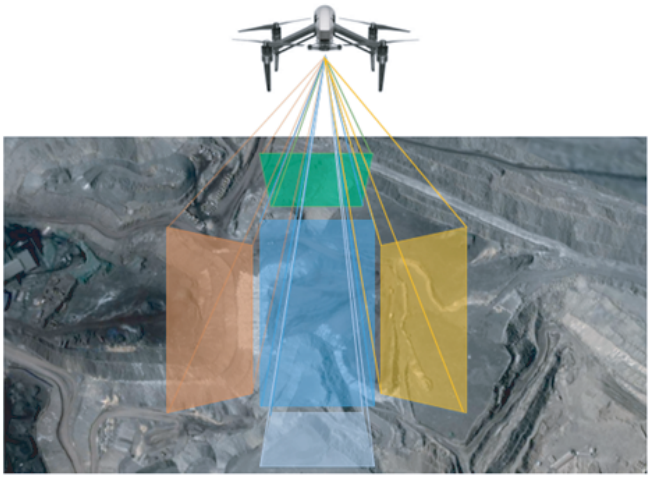

Figure 3. Schematic diagram of tilt photogrammetry.

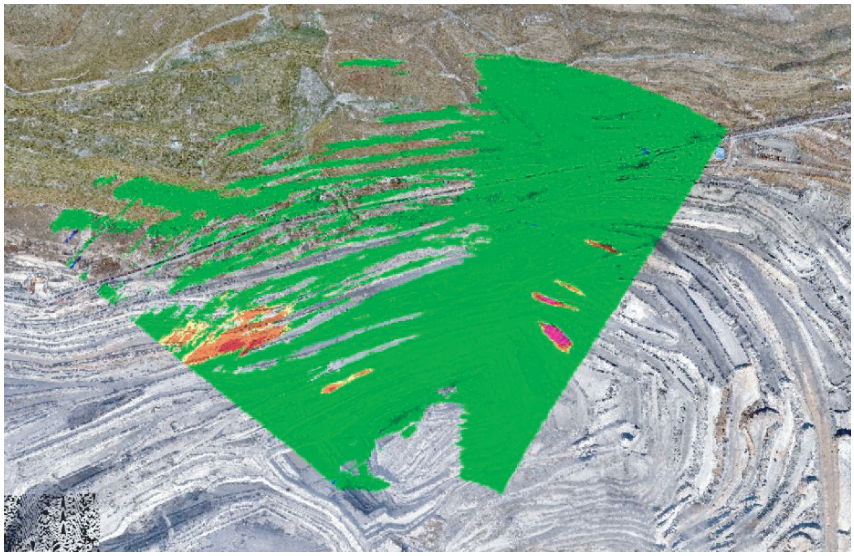

Figure 4. Radar data and 3D data fusion diagram.

In order to obtain the objective function, the deformation field needs to be surface fitted.

3.2. Momentum Gradient Descent Method

It is generally believed that the direction with the largest change of cumulative deformation displacement and deformation velocity is the main sliding direction of landslide. In many actual landslide cases, the main sliding direction of landslide is also the direction with the largest displacement gradient. From a mathematical point of view, the direction of gradient is the direction of the fastest growth of the function, and the reverse direction of gradient is the direction of the fastest reduction of the function. Therefore, in actual monitoring, the main sliding direction of landslide can be determined by solving the gradient of deformation scalar field. At present, some scholars have applied the gradient descent method to determine the main sliding direction of the landslide. Its basic idea can be simply described as follows: take the maximum deformation point as the starting point p_0, find the direction of the steepest decline relative to this position, that is, the reverse direction of the gradient, move a distance along this direction to get point p_1, repeat the first step to get point p_2 with point p_1 as the starting

point, and then cycle step by step until convergence, and a series of p points will be obtained. The line between p_0 and p_n is considered as the main sliding direction of the landslide. The specific method is described below.

Given the initial point $p_0(x_0, y_0, z_0)$ in the scalar field $f(x, y, z)$, it can be obtained from the directional derivative:

$$\begin{aligned}\frac{\partial f}{\partial l} &= \frac{\partial z}{\partial x}\cos\alpha + \frac{\partial z}{\partial y}\cos\beta + \frac{\partial z}{\partial z}\cos\gamma = \left(\frac{\partial z}{\partial x}, \frac{\partial z}{\partial y}, \frac{\partial z}{\partial z}\right)\cdot(\cos\alpha, \cos\beta, \cos\gamma) \\ &= G \cdot e_1 = |G|\cdot|e_1|\cos(G, e_1) = |G|\cos(G, e_1) \end{aligned} \tag{9}$$

where $\frac{\partial f}{\partial l}|_{p_0}$ is the rate of change of the surface along the direction l at point p_0. When $\cos(G, e_1)$ is 1, the directional derivative can get the maximum value $|G|$, and G is usually called the gradient at point p_0, which is recorded as:

$$\nabla f(x, y, z) = gradf(x, y, z) = \frac{\partial f}{\partial x}i + \frac{\partial f}{\partial y}j + \frac{\partial f}{\partial z}k \tag{10}$$

Since the negative gradient direction is the case where the function decreases the fastest, the iteration formula is as follows:

$$(x_{i+1}, y_{i+1}) \leftarrow (x_i, y_i) + \eta p_{\mathrm{d}} \quad i \geq 0 \tag{11}$$

Among them, p_{d} is the search direction, $p_{\mathrm{d}} = -\nabla f(x, y)$ the negative gradient direction, and η the step size. In order to ensure the accuracy of the descent path, the general step size should not be too large. It is worth noting that in order to move one step at a time and find its local minimum value, it is very necessary to carry out surface fitting on the deformation field of the landslide. Therefore, z value is a fitting value and does not necessarily exist in the terrain field, so only x and y are calculated in the above formula, and then z value is determined in the digital terrain model (DSM) based on the obtained x and y values. Namely:

$$z_{(i+1)} = H(x_{(i+1),}y_{(i+1)}, t) \quad i \geq 0 \tag{12}$$

Since most landslide directions are the same as the slope inclination direction, if the previous descending direction is taken into account, the oscillation will be reduced. When the gradient descending direction is the same as the last updating amount, the last updating amount can play a positive acceleration role in this search. Therefore, in combination with the momentum idea in physics, the momentum term v and attenuation factor γ are introduced in the gradient descent solution process to guide the parameters to converge towards the optimal value faster. The iterative formula after introducing momentum is as follows:

$$\begin{aligned} v_{i+1} &\leftarrow \gamma v_i + \eta p_{\mathrm{d}} \\ (x_{i+1}, y_{i+1}) &\leftarrow (x_i, y_i) + v_{i+1} \end{aligned} \tag{13}$$

where γ represents the influence of historical gradient. If the gradient at the current moment approaches the direction of historical gradient, this trend will be strengthened at the current moment; otherwise, the gradient direction at the current moment will be weakened. When v_i is consistent with the negative gradient direction, the algorithm efficiency can be effectively improved.

4. DISPLACEMENT ALONG SLOPE DIRECTION

4.1. Joint Calculation of Ground Inclination and Radar Incidence Angle

The precise geometric relationship of micro-variation monitoring radar observation is shown in Figure 5. In the figure, r represents the true value of landslide deformation, r_{defo} the LoS-direction displacement, τ the radar incidence angle, φ the slope angle between the landslide direction and the ground, and θ the mapping angle between the true value of deformation and the LoS-direction displacement. According to the geometric relationship, $\theta = \frac{\pi}{2} - \varphi + \tau$, it can be seen from Equation (12) that the solution of the true value of landslide deformation is related to the radar incidence angle and the ground inclination angle. In practical application, the ground inclination often needs to be measured manually, which

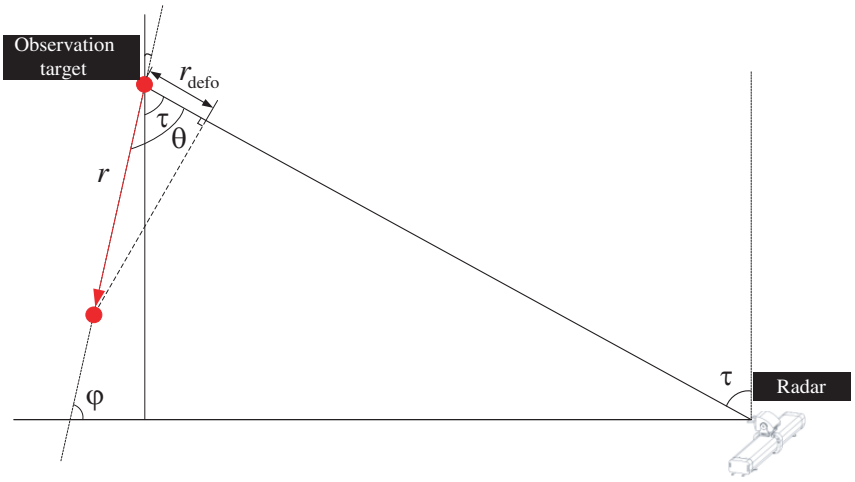

Figure 5. Schematic diagram of the precise geometric relationship of radar observation.

cannot automatically calculate the true value of landslide deformation. This method is invalid in areas where people cannot reach.

$$r = \frac{r_{\text{defo}}}{\sin(\tau - \varphi)} = \frac{r_{\text{defo}}}{\cos\theta} \tag{14}$$

4.2. Joint Calculation of LoS Displacement and Main Sliding Direction

The determination of landslide displacement direction is relatively complex and is often determined according to the landform. Generally, the main sliding direction of the landslide is the line between the highest and most convex point on the back wall, the farthest and outermost convex point pushed out by the front edge of the landslide mass, and the deepest point on the upper and lower concave of the cross section after the landslide. In addition, through displacement monitoring, the plane resultant displacement vector curve of the landslide in a period of time can be obtained to determine the direction of the landslide, and the landslide direction is basically consistent with the slope direction when most slope surfaces are unstable. As a non-contact monitoring method, the micro-variation monitoring radar can obtain high-resolution radar images and million-level monitoring points through spatial scanning. Therefore, the use of the micro-variation monitoring radar can obtain the main sliding direction information of landslide more conveniently and accurately. In literature, the deformation field and terrain field are fused, and then local surface fitting is performed. Finally, gradient descent is used to realize the identification and prediction of the main sliding direction of the landslide.

The included angle between the slope displacement direction and the ENU direction (see Figure 6) is set as the sliding azimuth μ. If it is 0° in the due north direction, each sliding azimuth angle μ clockwise represents a positive angle and counterclockwise represents a negative angle. Based on the information of the main sliding direction of the slope, the direction vector of the displacement along the slope direction can be solved, and the expression is obtained as follows:

$$\mu = arc\cos\frac{a \cdot b}{|a|\,|b|} = arc\cos\frac{(x_a, y_a, z_a) \cdot (x_b, y_b, z_b)}{\sqrt{x_a^2 + y_a^2 + z_a^2} \cdot \sqrt{x_b^2 + y_b^2 + z_b^2}} \tag{15}$$

In the above formula, vector a is the unit vector in the due north direction, and vector b is the direction vector of displacement along the slope direction. From the above formula:

$$x_b^2 + y_b^2 + z_b^2 = \frac{(x_a x_b + y_a y_b + z_a z_b)^2}{\cos^2\mu} \tag{16}$$

where z_b is the elevation of the last point displaced along the slope direction, which can be determined by the digital surface model (DSM). If x_b is assigned any non-zero constant, the value of y_b can be

determined, or vice versa. The positive and negative values of x_b or y_b depend on the relationship between the displacement direction along the slope and ENU. Since the LoS direction vector R is known, the mapping angle θ of the LoS direction and the displacement along the slope direction of any observation point can be obtained by combining the direction vector of the displacement along the slope direction. The expression is shown in the formula. According to the mapping relationship between the LoS direction displacement and the displacement along the slope direction in Section 2.2, the displacement along the slope direction can be calculated.

$$\theta = arc\cos\frac{b\cdot R}{|b|\,|R|} = arc\cos\frac{(x_b,y_b,z_b)\cdot(x_o-x_p,y_o-y_p,z_o-y_p)}{\sqrt{x_b^2+y_b^2+z_b^2}\cdot\sqrt{(x_o-x_p)^2+(y_o-y_p)^2+(z_o-y_p)^2}} \tag{17}$$

According to the relationship between LoS-direction displacement and its 3D projection component described in Section 3.2, and the mapping relationship between LoS-direction displacement and deformation truth value in Section 2.2, as shown in Figure 6, the relationship between landslide deformation truth value r and LoS-direction 3D projection can be obtained as follows:

$$r = \frac{\left|\overrightarrow{PP_{\mathrm{n}}}\right|}{\cos\theta_{\mathrm{n}}\cdot\cos\theta}, \quad n = 1,2,3 \tag{18}$$

In the above formula, $\left|\overrightarrow{PP_{\mathrm{n}}}\right|$ is the 3D projection component of the LoS direction, θ_n the included angle between the LoS direction and the ENU direction, and μ the main sliding direction of the landslide displacement.

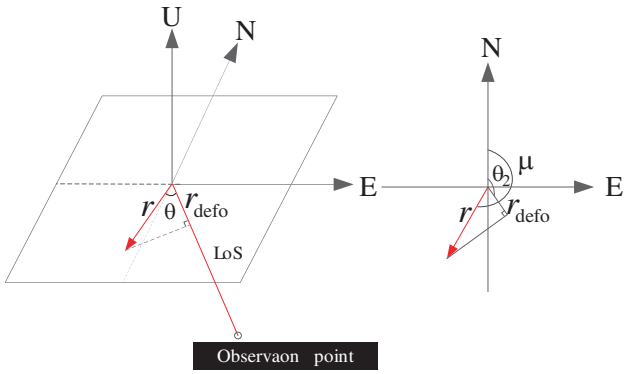

(a) Space projection (b) Horizontal projection

Figure 6. Schematic diagram of the mapping angle Theta solution.

5. VERIFICATION OF MEASURED DATA

5.1. Monitoring Area and Data Source

The experimental area is a slope, which is affected by continuous heavy rainfall. The argillaceous dolomite of the mountain softens when it meets water, and the top rock mass undergoes instability and collapse under the action of gravity. The top rock mass collapses under gravity. In order to prevent the secondary collapse from threatening the safety of rescue and rehabilitation workers, the LSA system of micro-variation monitoring radar is deployed on the site to monitor the process of landslide area treatment. According to the actual topographic conditions of the slope, the micro-variation monitoring radar monitoring station is selected at the stable position of the foundation on the opposite bank of the slope, and there is no obstacle between the equipment and the target slope, so the whole slope can be observed.

In order to ensure the stability of the equipment, the micro-variable monitoring radar is placed in the monitoring room, and the establishment of the monitoring room can effectively avoid the impact of adverse weather on the reliability of the monitoring results. During observation, the data acquisition

Table 1. Micro Deformation Monitoring Radar LSA system parameters.

Parameters	Numerical value	Parameters	Numerical value
frequency range	$16.5 \sim 17.5$ GHz	Monitoring range	$60°$(azi) $\times$ $30°$(ele)
Deformation monitoring accuracy	0.1 mm	Pulse repetition rate	≥ 500 Hz
Operating distance	5 km	Displacement observation period	$240 \sim 600$s
Image resolution	0.3 m $\times$ 0.0054 rad	Power supply	AC220 V/DC24 V
Total weight of equipment	≤ 150 kg	working temperature	$-30 \sim 50°$C

Figure 7. Micro Deformation Monitoring Radar LSA monitoring system.

interval is 10 min; the range resolution is 0.3 m; and the azimuth resolution is 0.0054 rad. Figure 7 shows the LSA system of the micro change monitoring radar used, and its system parameters are shown in Table 1.

5.2. Data Processing and Analysis

In a large range of incidence angle, the trihedral corner reflector can reflect the incident electromagnetic wave in the opposite direction, thus having a strong backscattering cross section (RCS). The electromagnetic wave will produce strong reflection on the metal corner reflector and then be received by the radar receiver. After radar imaging processing, strong targets will appear on the radar image. Therefore, the accurate location information and deformation information of the monitoring point can be obtained through the corner reflector [17–20]. In this paper, a trihedral corner reflector composed of three mutually perpendicular flat plates is selected as the experimental device. As shown in Figure 8, the normal direction of the center of the trihedral corner reflector is within the range of radar line of sight, and the radar echo intensity results of the corner reflector placement area are shown in Figure 9.

The corner reflector moves 7 times, including the first 4 times moving 10 mm each time, and the last 3 times moving 30 mm each time, collecting 2 pieces of data each time. PP' is the direction of the landslide in the observation area, and it will be lifted by a certain distance along the direction of PP' each time.

Through the acquired UAV point cloud data, we can obtain the three-dimensional spatial geographic coordinates of the radar and the angle reversal point, as shown in Table 2.

According to the 3D deformation acquisition method of LoS displacement described in Section 3.2, the included angle between LoS displacement and due north direction can be obtained, that is $\theta_2 = 104.9°$. According to the field experimental goniometer, the included angle $\mu = 20.8°$ between the angle reverse movement direction and the due north direction is obtained. Using the method described in Section 4.2, the included angle $\theta = 84.1°$ between the line-of-sight displacement and the

Figure 8. Experimental trihedral corner reflector device.

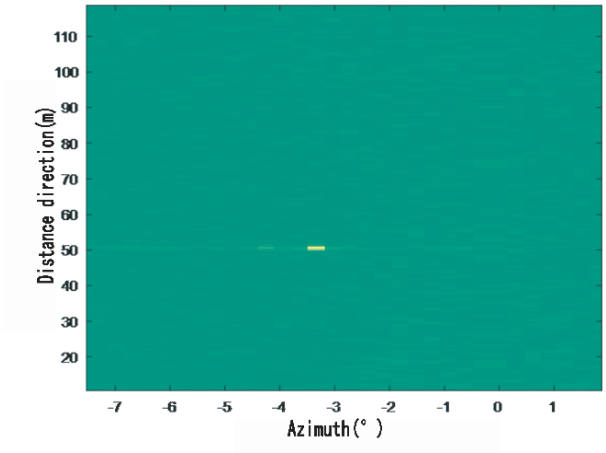

Figure 9. Radar echo intensity map of corner reflector placement area.

Table 2. Radar and corner reflector three-dimensional geographic coordinates.

project	x	y	z
radar	505310.3523	3213634.4785	1333.1455
Corner reflector	504442.4743	3213871.5924	1130.6392

Table 3. True value of landslide deformation.

Time	LoS displacement/mm	True value of deformation/mm
16:27:14	0.0488	0.4670
16:36:22	0.1173	1.1226
16:45:29	1.2085	11.5647
16:54:37	1.2335	11.8034
17:03:46	1.97148	18.8659
17:12:54	2.0374	19.4975
17:22:01	3.229	30.8977
17:31:09	3.2589	31.1865
17:40:17	4.2519	40.6881
17:49:24	4.2778	40.9359
17:58:30	7.3245	70.0906
18:07:37	7.4367	71.0963
18:16:45	10.6091	101.5225
18:25:52	10.6091	101.5225

landslide deformation displacement mapping can be obtained, and the relationship between the landslide deformation displacement r and the apparent displacement r_{defo} is obtained as follows:

$$r_{\text{defo}} = r * \cos(84.1^\circ) \tag{19}$$

According to the above formula, the true values of LoS displacement and landslide deformation are shown in Table 3.

In order to illustrate the effectiveness of the method for calculating the deformation truth value proposed in this paper, the calculated deformation truth value results are compared with the actual displacement results of the trihedral corner reflector, as shown in Figure 10. The calculated result and the actual moving distance are compared. Figure 11 shows the comparison result. The closer the curve is to 0, the more accurate the calculated result is. Two pieces of data are collected for each movement. The first movement can capture the angular inverse movement, and the deformation value is relatively large, while the angular inverse is stable in the course of the second acquisition, so the deformation value has no obvious change, which is reflected in the data as a curve ladder rise.

It can be seen from Figure 10 and Figure 11 that the deformation displacement in the direction of the landslide and the actual lifting displacement of the corner reflector present the same trend, with the root mean square error of 1.1379 mm and the maximum error of 1.8034 mm. Considering that the experiment is conducted outdoor, the noise signal in the monitoring process will interfere with the final calculation results. But on the whole, the displacement trends of the two are basically the same, which verifies the effectiveness of the method proposed in this paper to solve the true value of landslide deformation.

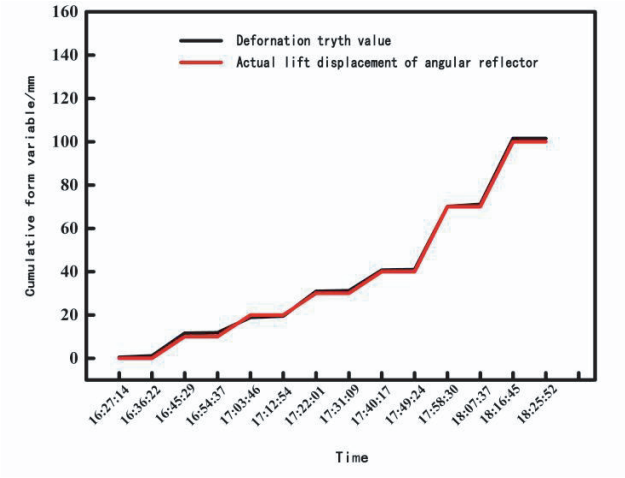

Figure 10. Comparison diagram of cumulative deformation displacement and actual lifting displacement.

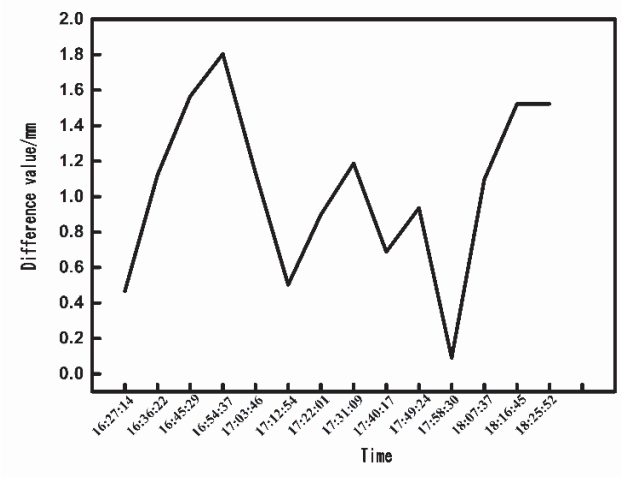

Figure 11. Deformation difference graph.

6. CONCLUSION

In view of the fact that the micro-variation monitoring radar can only observe a single LoS-direction displacement, this paper proposes a method to calculate the true value of landslide deformation. Firstly, based on three-dimensional geographic coordinates, the LoS-direction displacement is analyzed in three dimensions. Then, the mapping angle between the line of sight displacement and the landslide direction is solved by combining the landslide direction. Finally, according to the mapping relationship between the LoS-direction displacement of radar and the true value of deformation, the deformation displacement of landslide direction is calculated. Taking a slope as the study area, the feasibility and effectiveness of the method are verified by the measured data.

The method proposed in this paper is universal in principle, can adapt well to a variety of monitoring situations, and can realize automatic calculation of deformation truth value, which has certain reference value in practical applications. However, when the direction of landslide is determined in practical engineering, for different slope geological conditions, it is necessary to select a reasonable method to ensure the accuracy of calculating the mapping angle of LoS displacement and landslide direction.

REFERENCES

1. Fang, Z., "National geological hazard bulletin[OL]," Jun. 2020 (in Chinese), http://www.cgs.gov.cn/gzdt/zsdw/202003/t20200331_504559.html.
2. Zeng, T., Y. Deng, C. Hu, et al., "Development state and application examples of ground-based differential interferometric radar," *Journal of Radars*, Vol. 8, No. 1, 154–170, 2019 (in Chinese).
3. Liu, B., D. Ge, M. Li, et al., "Ground-based interferometric synthetic aperture radar and its applications," *Remote Sensing for Land and Resources*, Vol. 29, No. 1, 1–6, 2017 (in Chinese).
4. Du, L., "Study about instability criterion and deformation prediction of rock slope based on fractal theory," China University of Geosciences (Beijing), 2020 (in Chinese).
5. Zeng, T., C. Mao, C. Hu, and W. Tian, "Ground-based SAR wide view angle full-field imaging algorithm based on keystone formatting," *IEEE Journal of Selected Topics in Applied Earth Observations and Remote Sensing*, Vol. 9, No. 6, 2160–2170, 2016.
6. Li, Z., J. Wang, Q. H. Liu, et al., "Frequency-domain backprojection algorithm for synthetic aperture radar imaging," *IEEE Geosc. and Remote Sensing Letters*, Vol. 12, No. 4, 905–909, 2015.
7. Tarchi, D., N. Casagli, R. Fanti, et al., "Landslide monitoring by using ground-based SAR interferometry: An example of application to the Tessina landslide in Italy," *Engineering Geology*, Vol. 68, Nos. 1–2, 15–30, 2003.
8. Kuraoka, S., Y. Nakashima, R. Doke, et al., "Monitoring ground deformation of eruption center by ground-based interferometric synthetic aperture radar (GB-InSAR): A case study during the 2015 phreatic eruption of hakone volcano open access," *Earth, Planets and Space*, Vol. 70, 181, 2019.
9. Lombardi, L., M. Nocentini, W. Frodella, et al., "The Calatabiano landslide (southern Italy): Preliminary GB-InSAR monitoring data and remote 3D mapping," *Landslides*, Vol. 14, No. 2, 685–696, 2017.
10. Qi, L., W. Tan, P. Huang, et al., "Landslide prediction method based on a ground-based micro-deformation monitoring radar," *Remote Sensing*, Vol. 12, No. 8, 1230, 2020.
11. Qu, S., Y. Wang, W. Tan, et al., "Deformation detection error analysis and experiment using ground based SAR," *Journal of Electronics & Information Technology*, Vol. 33, No. 1, 1–7, 2011 (in Chinese).
12. Antonello, G., D. Tarchi, N. Casagli, et al., "SAR interferometry from satellite and ground-based system for monitoring deformations on the Stromboli volcano," *IEEE International Geoscience & Remote Sensing Symposium*, 636, 2004.
13. Bardi, F., F. Raspini, A. Ciampalini, et al., "Space-borne and ground-based InSAR data integration: The Åknes test site," *Remote Sensing*, Vol. 8, No. 3, 237, 2016.
14. Carlà, T., E. Intrieri, F. Raspini, et al., "Perspectives on the prediction of catastrophic slope failures from satellite InSAR," *Scientific Reports*, Vol. 9, No. 1, 14137, 2019.
15. Caduff, R., F. Schlunegger, A. Kos, et al., "A review of terrestrial radar interferometry for measuring surface change in the geosciences," *Earth Surface Processes and Landforms*, Vol. 40, No. 2, 208–228, 2015.
16. Atzeni, C., M. Barla, M. Pieraccini, et al., "Early warning monitoring of natural and engineered slopes with ground-based synthetic-aperture radar," *Rock Mechanics and Rock Engineering*, Vol. 48, No. 1, 235–246, 2015.
17. Wright, T. J., B. Parsons, P. C. England, et al., "InSAR observations of low slip rates on the major faults of western tibet," *Science*, Vol. 305, No. 5681, 236–239, Jul. 9, 2004.
18. Song, Y., "Estimating large gradient ground deformation with dinsar and offset-tracting," Southwest Jiaotong University, Chengdu, 2016 (in Chinese).
19. Jiang, L., K. Yang, and L. Che, "Monitoring of 3D deformation of target by ground-based synthetic aperture radar," *Surveying and Mapping Bulletin*, No. 3, 35–38, 2020 (in Chinese).
20. Huang, R., L. Jiang, X. Shen, et al., "An efficient method of monitoring slow-moving landslides with long-range terrestrial laser scanning: A case study of the Dashu landslide in the Three Gorges Reservoir Region, China," *Landslides*, Vol. 16, No. 3, 839–855, 2019.